A new high-capacity metal ion-complexing gel containing cyclen ligands

Ciarán Dolan[a,b], Fleur Drouet[a], David Ware[a], Penelope J. Brothers[a,b], Jianyong Jin[a,b], Margaret A. Brimble[a,b] and David E. Williams[a,b*]

[a] *School of Chemical Sciences, University of Auckland, Private Bag 92019, Auckland 1142, New Zealand*

[b] *The MacDiarmid Institute for Advanced Materials and Nanotechnology, Victoria University of Wellington, PO Box 600, Wellington 6140, New Zealand.*

Corresponding author: Tel: +64 9 9239877, e-mail address: david.williams@auckland.ac.nz

Supplementary Information

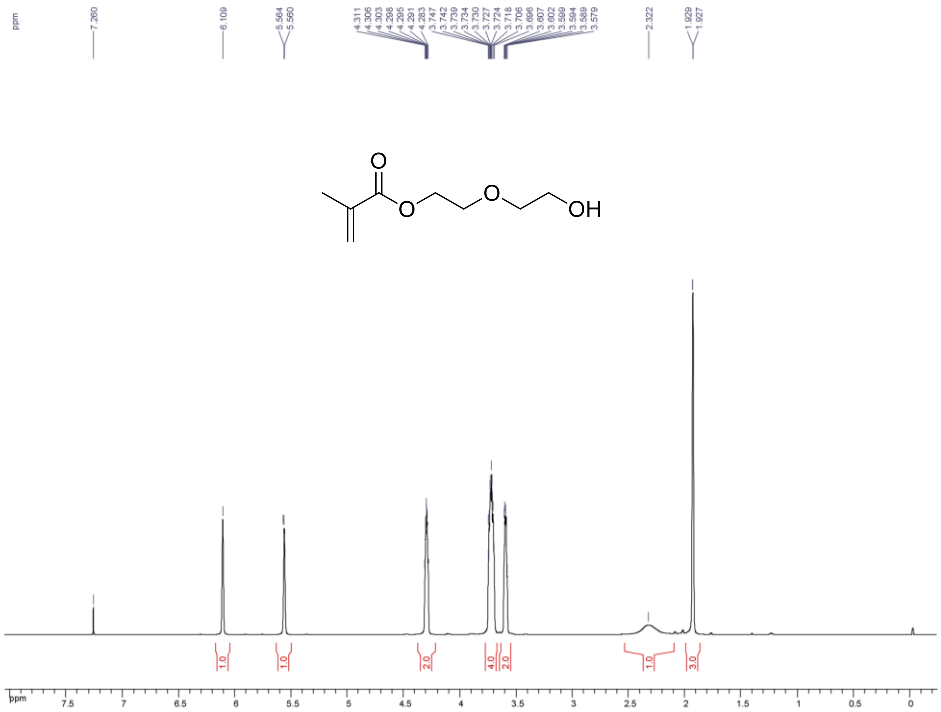

Fig. S1: ^{1}H NMR (400 MHz, $CDCl_3$) of 2-(2-hydroxyethoxy)ethyl methacrylate.

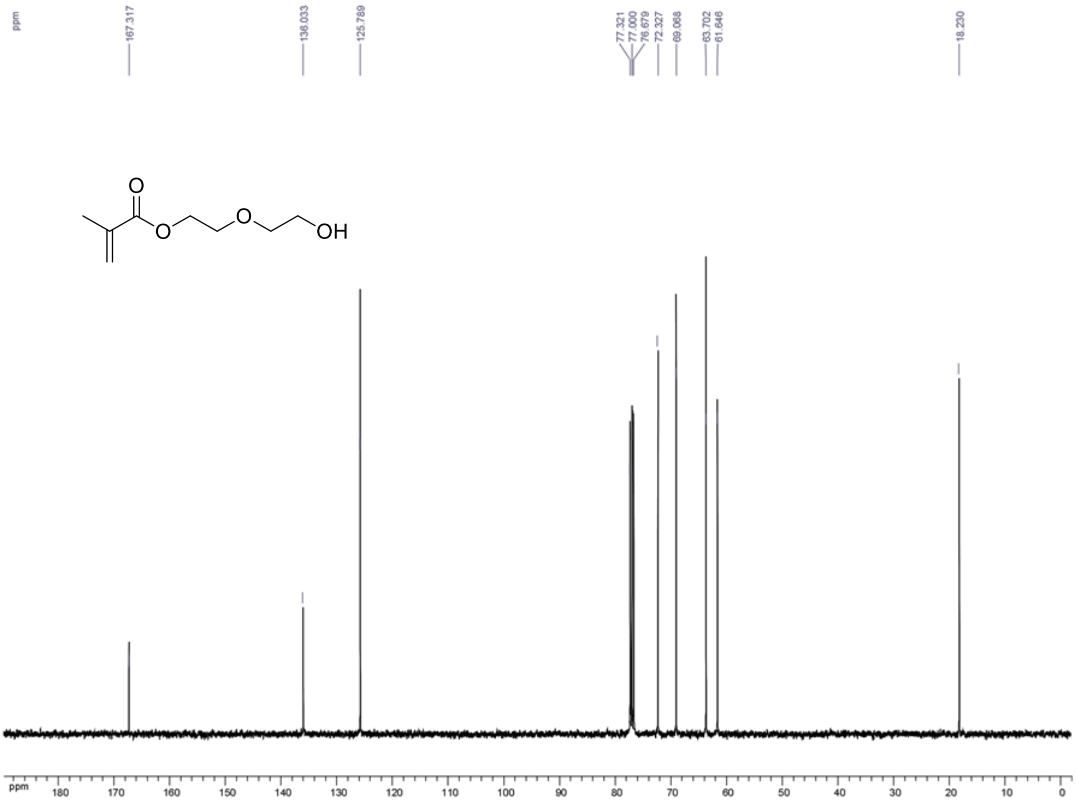

Fig. S2: ^{13}C NMR (100 MHz, $CDCl_3$) of 2-(2-hydroxyethoxy)ethyl methacrylate.

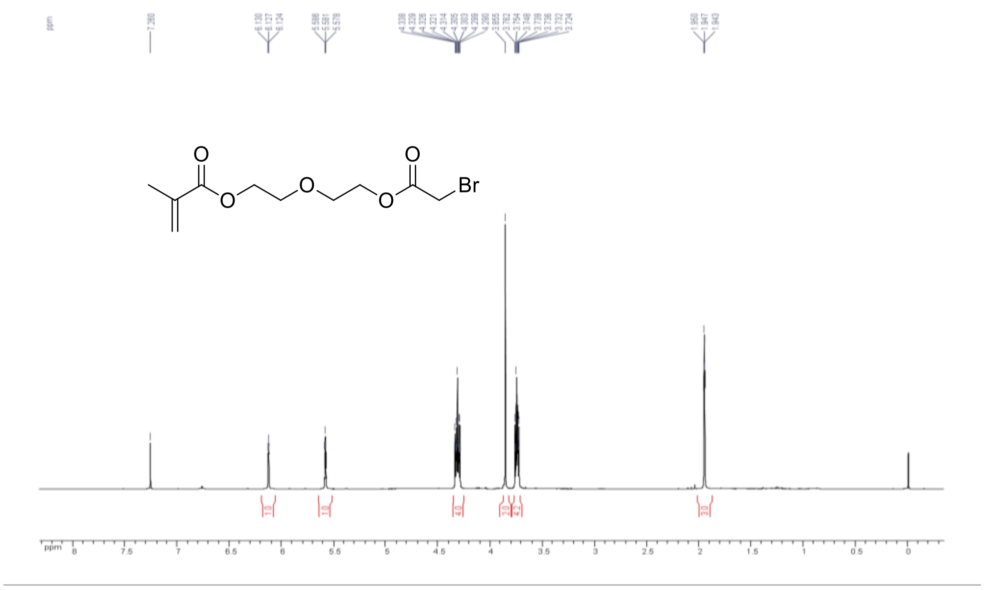

Fig. S3: ^{1}H NMR (400 MHz, $CDCl_3$) of 2-(2-(2-bromoacetoxy)ethoxy)ethyl methacrylate **2.**

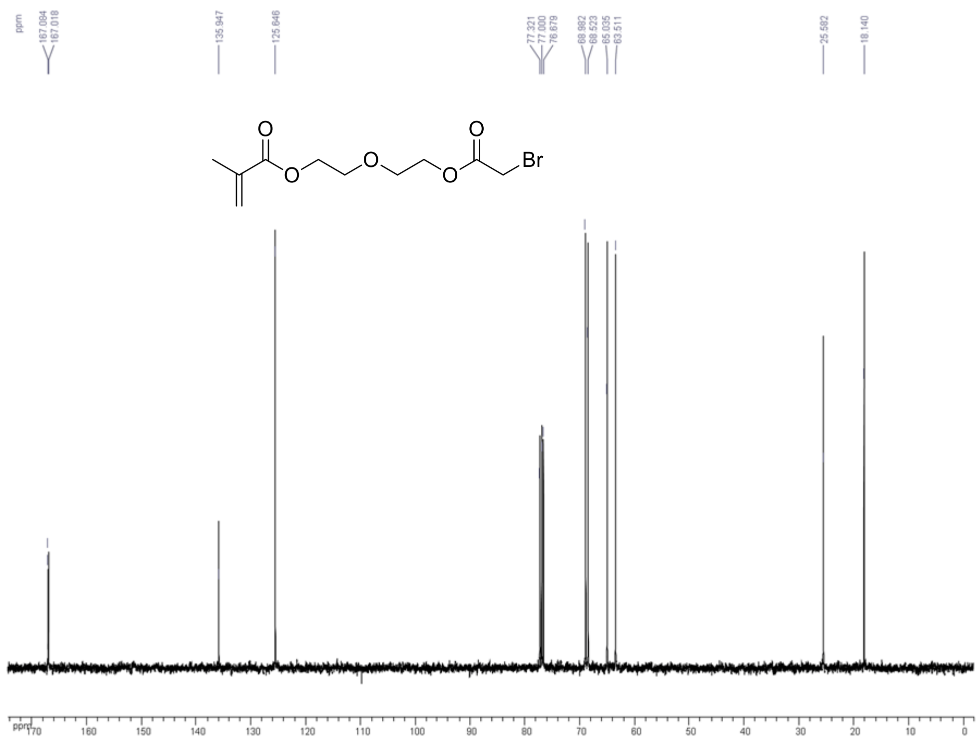

Fig. S4: ^{13}C NMR (100 MHz, $CDCl_3$) of 2-(2-(2-bromoacetoxy)ethoxy)ethyl methacrylate **2.**

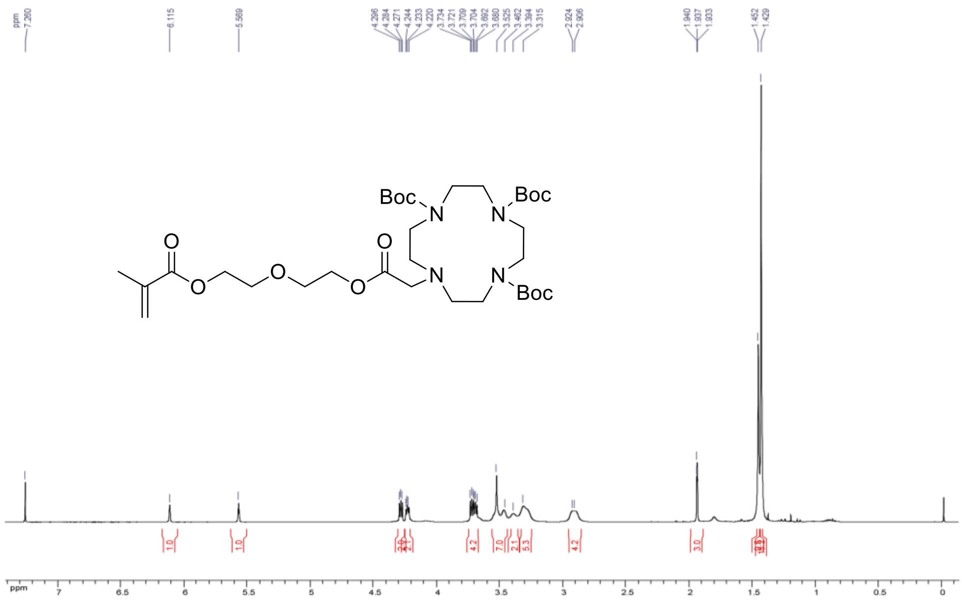

Fig. S5: ^{1}H NMR (400 MHz, $CDCl_3$) of 10-(2-(2-(2-(methacryloyloxy)ethoxy)ethoxy)-2-oxoethyl)-1,4,7,10- tetraazacyclododecane -1,4,7-tricarboxylate **1**.

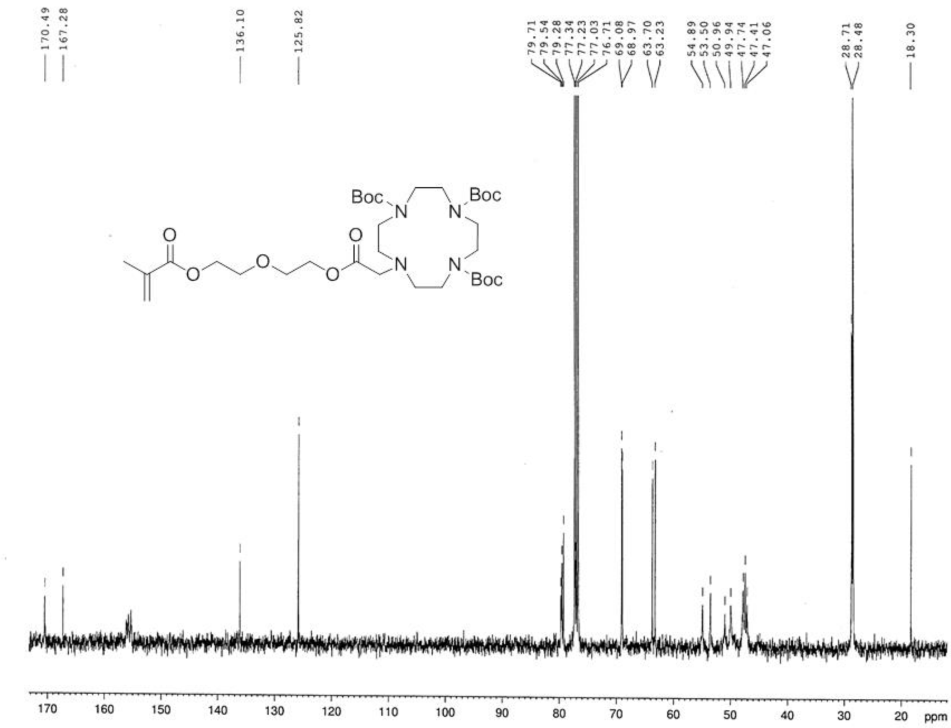

Fig. S6: ^{13}C NMR (100 MHz, $CDCl_3$) of 10-(2-(2-(2-(methacryloyloxy)ethoxy)ethoxy)-2-oxoethyl)-1,4,7,10- tetraazacyclododecane -1,4,7-tricarboxylate **1.**

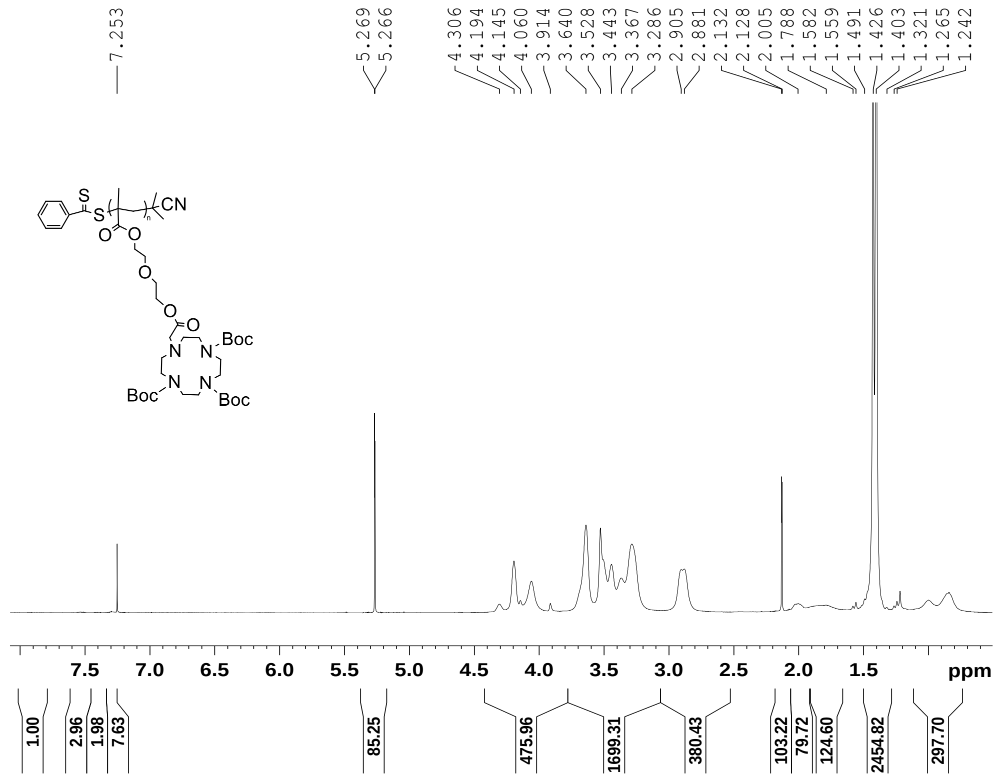

Fig. S7: ^{1}H NMR (400 MHz, $CDCl_3$) of **3-Boc**.

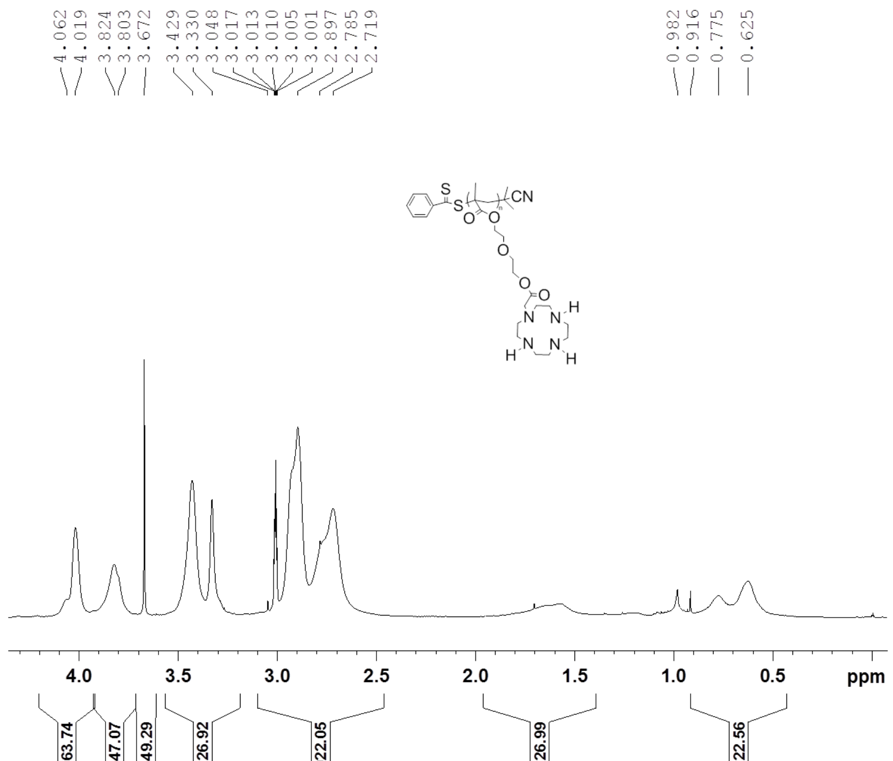

Fig. S8: ^{1}H NMR (400 MHz, acetone-d_6) of **3.**

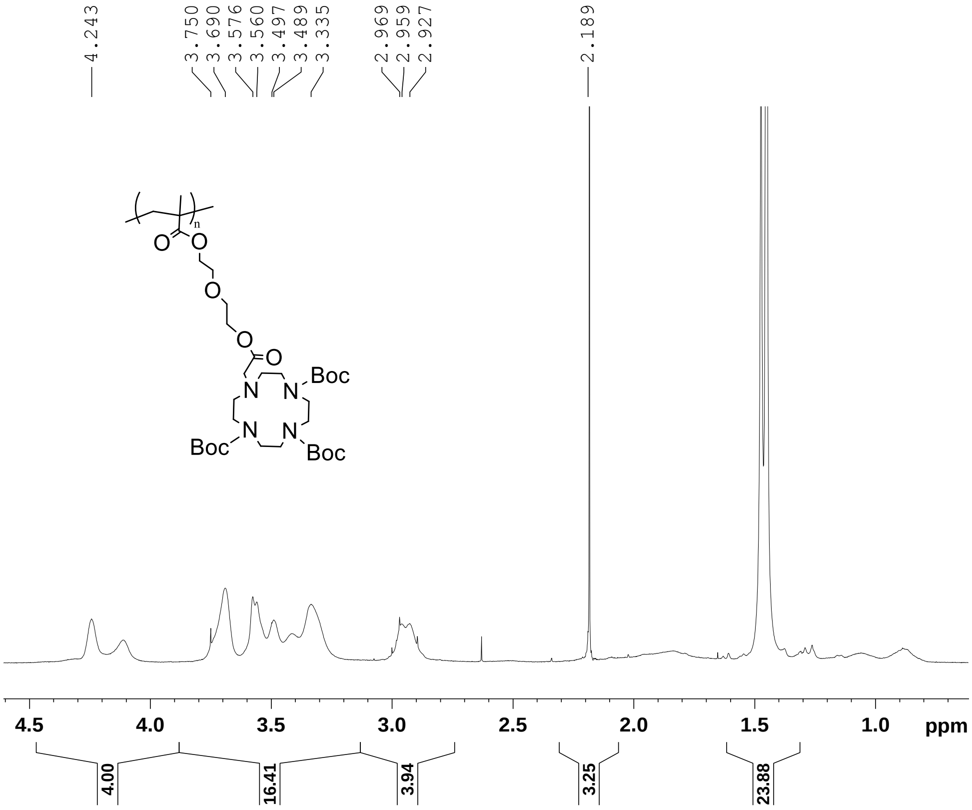

Fig. S9: ^{1}H NMR (400 MHz, $CDCl_3$) of **4-Boc**.

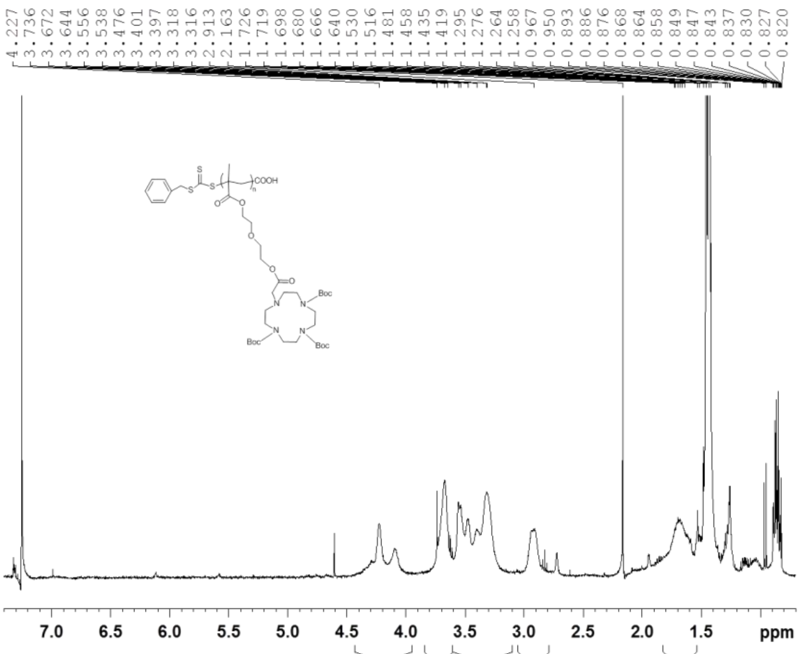

Fig. S10: ^{1}H NMR (400 MHz, $CDCl_3$) of **5-Boc**.

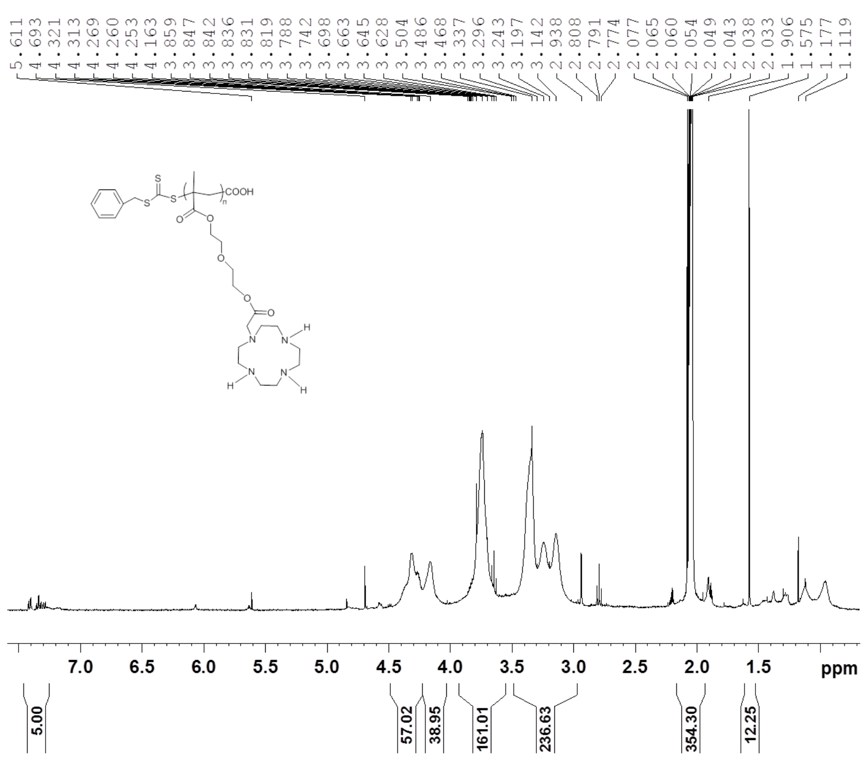

Fig. S11: ^{1}H NMR (400 MHz, acetone-d_6) of **5.**

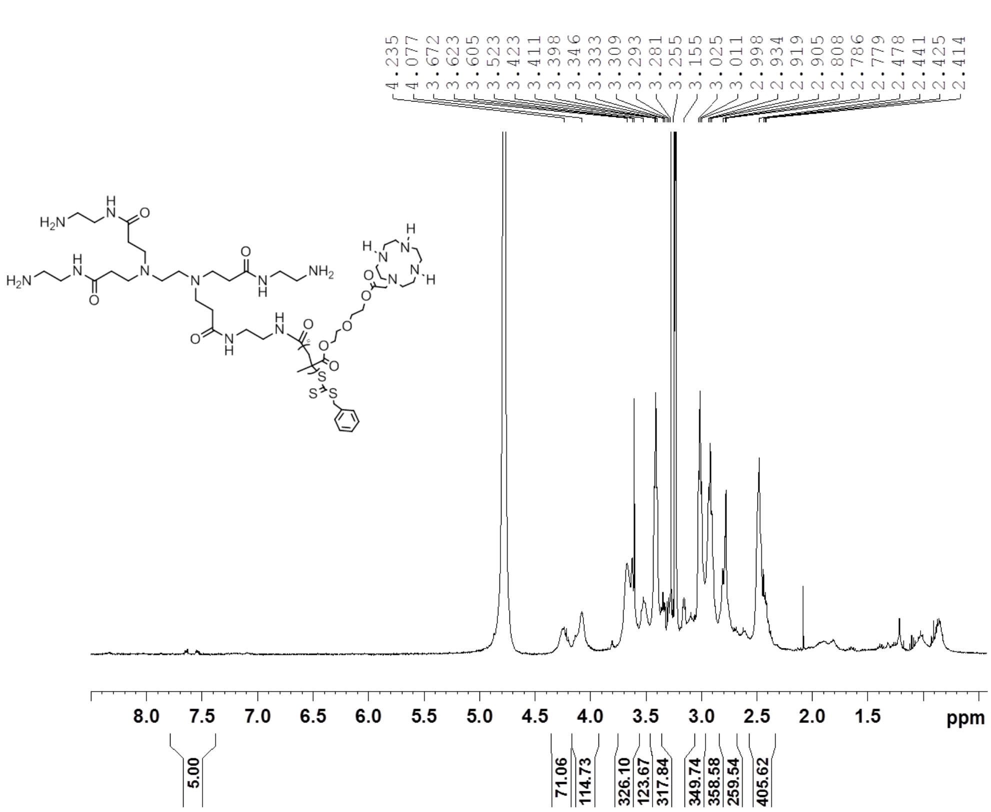

Fig. S12: ^{1}H NMR (400 MHz, CD_3OD-d_4) of ***5***-PAMAM (G0).

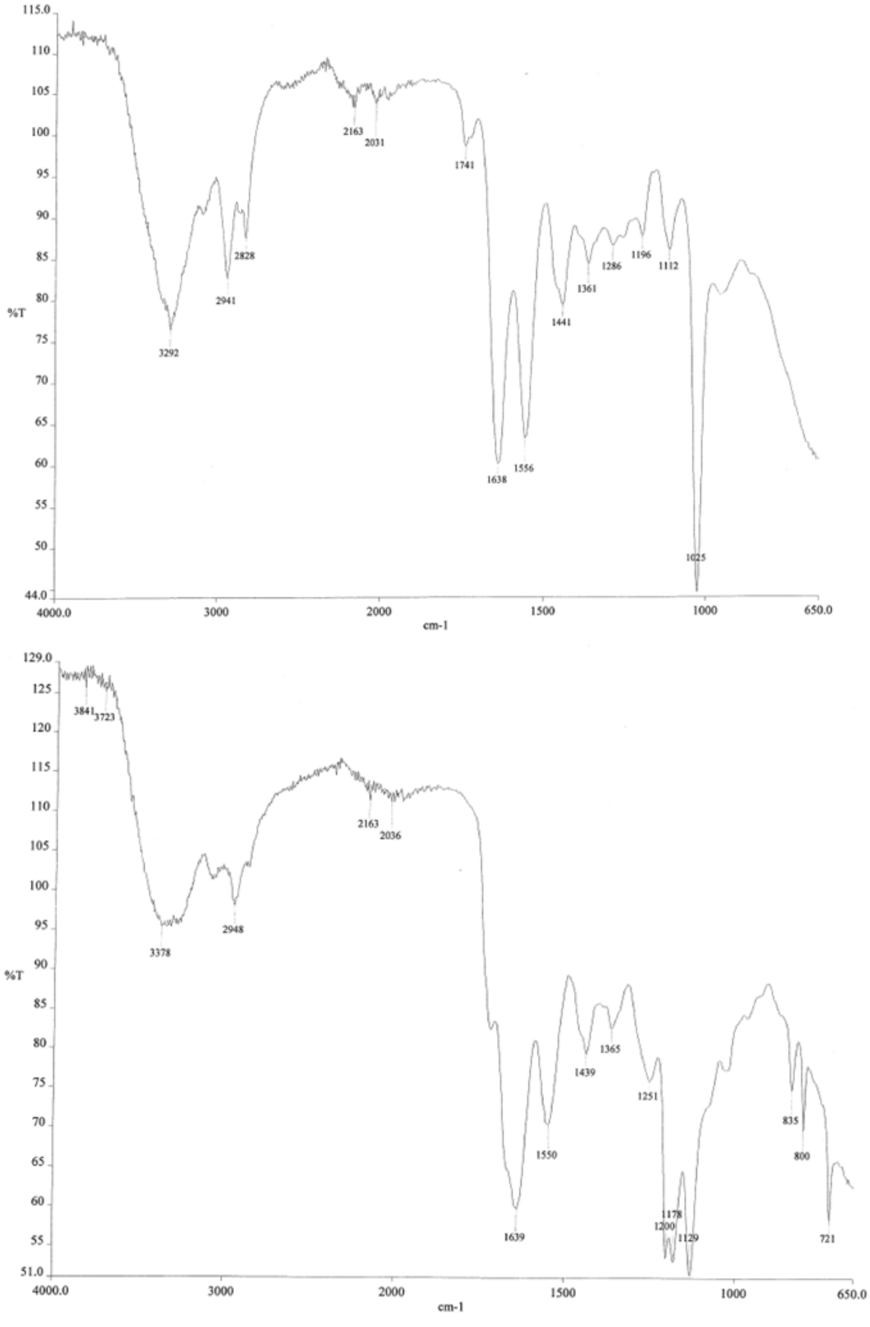

Fig. S13: FTIR spectrum of Cu-crosslinked-PAMAM (G0) (top) and Cu-crosslinked-5-PAMAM (G0) (bottom).

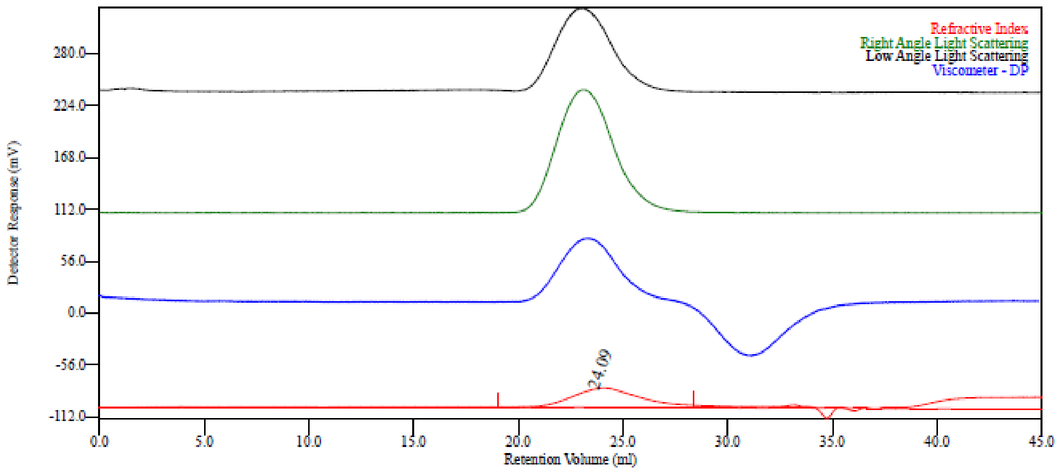

Multi-Detectors - Homopolymers : Results

Peak RV - (ml)	24.087
Mn - (Daltons)	111,721
Mw - (Daltons)	236,626
Mz - (Daltons)	381,651
Mp - (Daltons)	207,889
Mw / Mn	2.118
Percent Above Mw: 0	100.000
Percent Below Mw: 0	0.000
IV - (dl/g)	0.2743
Rh(w) - (nm)	9.543
Rg(w) - (nm)	No Calc
Wt Fr (Peak)	1.000
Mark-Houwink a	0.778
Mark-Houwink logK	-4.717
Branches	0.000
Branch Freq.	0.000
RI Area - (mvml)	77.33
UV Area - (mvml)	0.00
RALS Area - (mvml)	417.74
LALS Area - (mvml)	254.90
IVDP Area - (mvml)	221.31

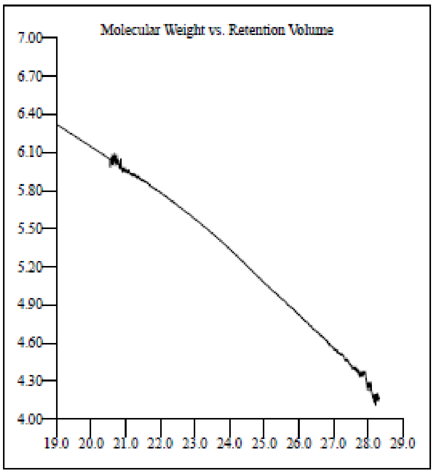

Annotation	
Method File	Metallo polymers-0003.vcm
Limits File	
Date Acquired	Jun 04, 2014 - 15:58:53
Solvent	THF
Acquisition Operator	admin : Administrator
Calculation Operator	admin : Administrator
Column Set	3 x T6000M
System	System 1
Flow Rate - (ml/min)	1.000
Inj Volume - (ul)	100.0
Volume Increment - (ml)	0.00333
Detector Temp. - (deg C)	35.0
Column Temp. - (deg C)	35.0
OmniSEC Build Number	406

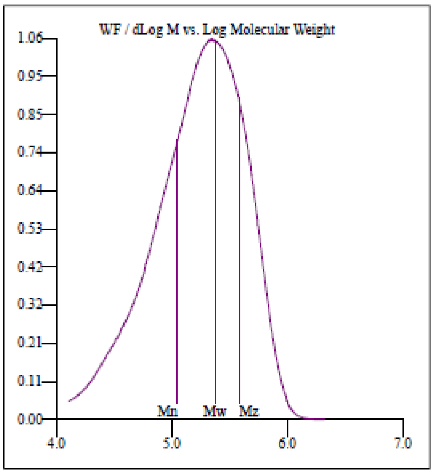

Fig. S14: GPC analysis of 235K Dalton polystyrene standard.

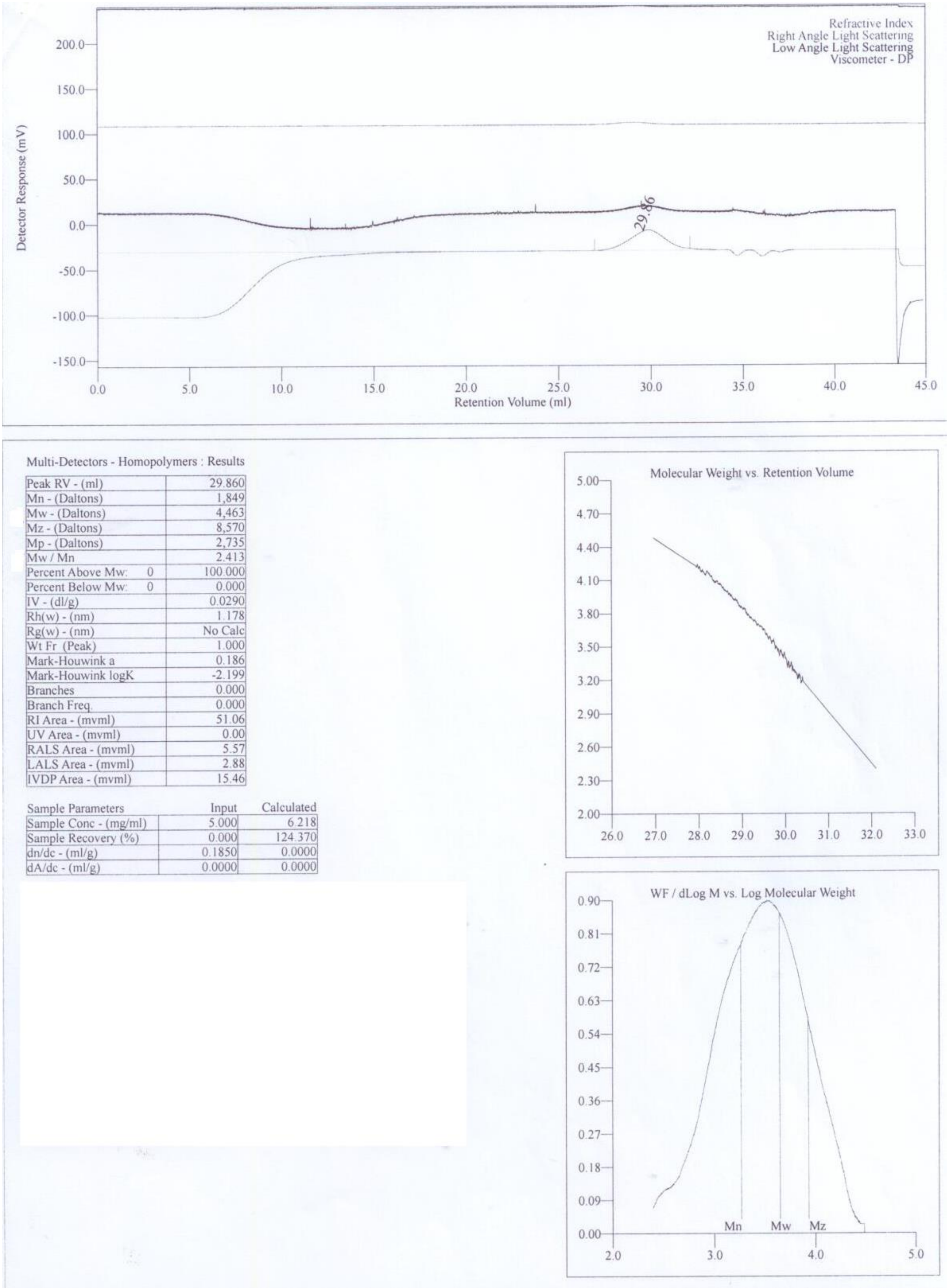

Multi-Detectors - Homopolymers : Results

Peak RV - (ml)	29.860
Mn - (Daltons)	1,849
Mw - (Daltons)	4,463
Mz - (Daltons)	8,570
Mp - (Daltons)	2,735
Mw / Mn	2.413
Percent Above Mw: 0	100.000
Percent Below Mw: 0	0.000
IV - (dl/g)	0.0290
Rh(w) - (nm)	1.178
Rg(w) - (nm)	No Calc
Wt Fr (Peak)	1.000
Mark-Houwink a	0.186
Mark-Houwink logK	-2.199
Branches	0.000
Branch Freq.	0.000
RI Area - (mvml)	51.06
UV Area - (mvml)	0.00
RALS Area - (mvml)	5.57
LALS Area - (mvml)	2.88
IVDP Area - (mvml)	15.46

Sample Parameters	Input	Calculated
Sample Conc - (mg/ml)	5.000	6.218
Sample Recovery (%)	0.000	124.370
dn/dc - (ml/g)	0.1850	0.0000
dA/dc - (ml/g)	0.0000	0.0000

Fig. S15: Example of GPC analysis; **4-Boc** polymer.

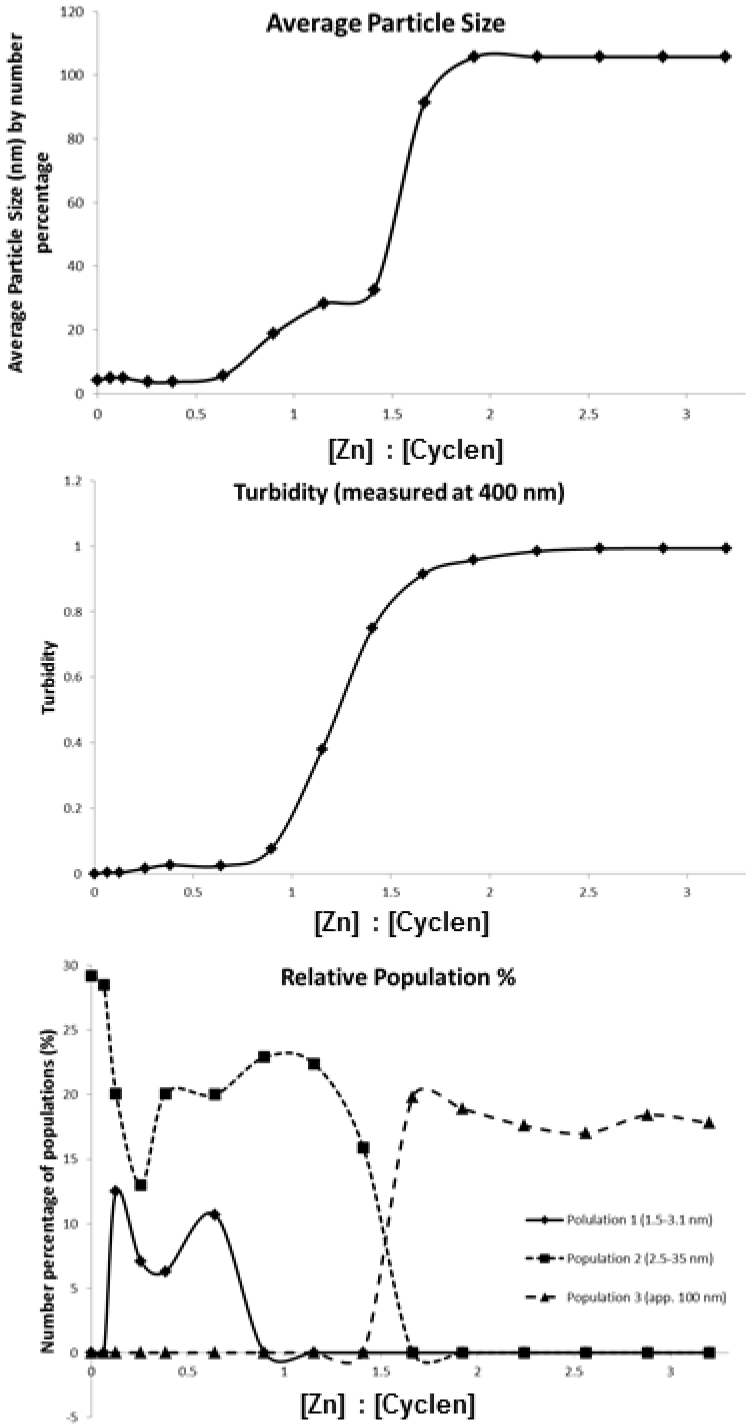

Fig. S16: Dynamic light scattering analysis monitoring the self-assembly of the **3-ZnCl$_2$** metallopolymer aggregates upon the dropwise addition of a solution of $ZnCl_2$ (in methanol) to polymer **3** in methanol; (top) average particle size; (middle) turbidity measurement; and (bottom) relative population percentage versus ratio of zinc to cyclen moieties on the polymer chain.

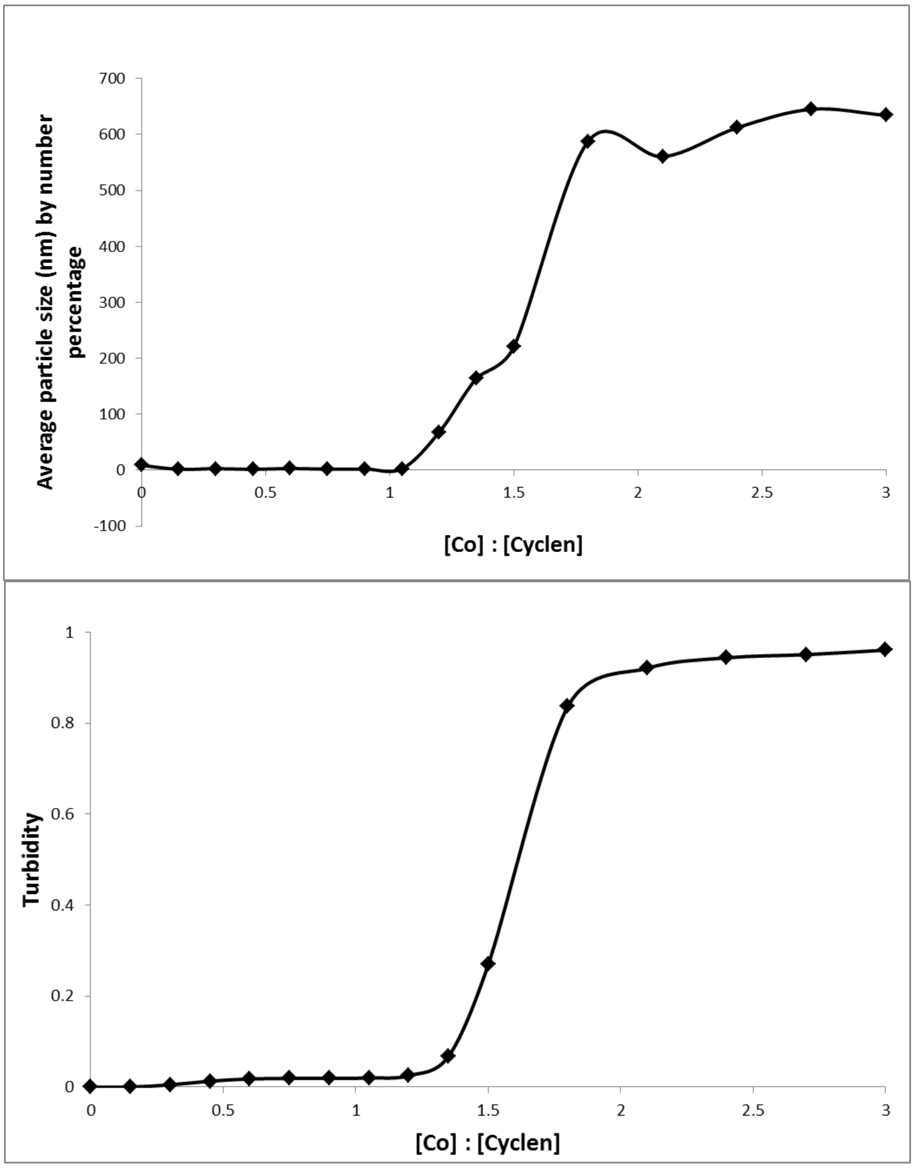

Fig. S17: (Top) Average particle size and (bottom) turbidity measurement versus ratio of cobalt to cyclen moieties on the polymer chain, characterising the development of Co-metallopolymer aggregates **3-CoCl$_2$** upon the dropwise addition of a solution of $CoCl_2$ to the homopolymer **3** solution in MeOH.

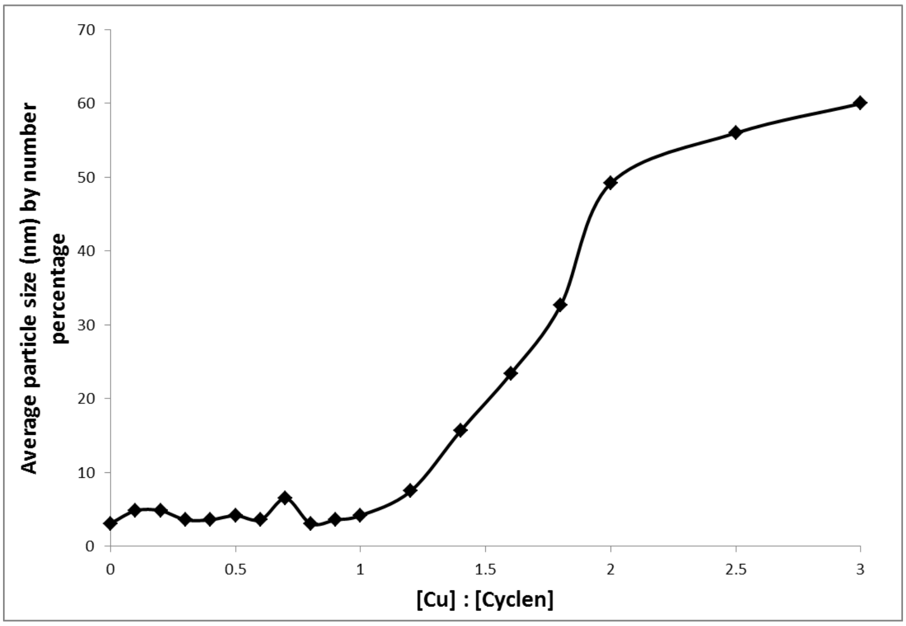

Fig. S18: Average particle size versus ratio of copper to cyclen moieties on the polymer chain, characterising the development of Cu-metallopolymer **3-CuCl$_2$** aggregates upon the dropwise addition of a solution of $CuCl_2$ to the homopolymer **3** solution in MeOH.

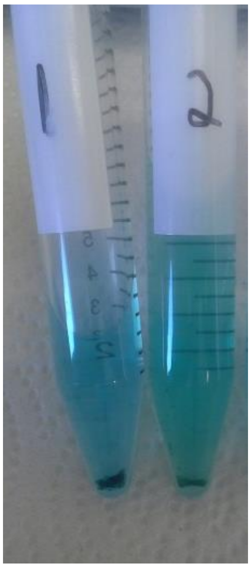

Fig. S19: Picture showing the precipitate formation of Cu-metallopolymers (1) **3-CuCl$_2$** and (2) **4-CuCl$_2$** after centrifugation at 1,500 rpm for 20 min.

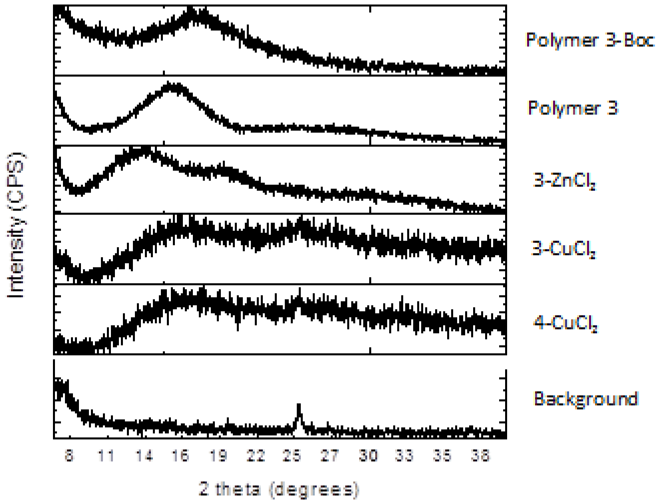

Fig. S20: Stacked XRD spectra of various polymers, metallopolymers and background.

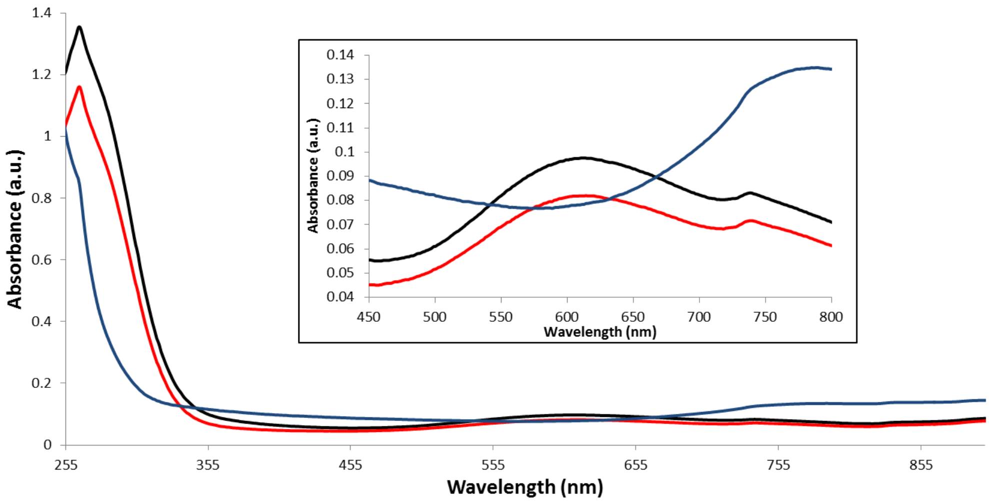

Fig. S21: UV-Visible absorption spectra of copper metallopolymers **3-CuCl$_2$** (black), **4-CuCl$_2$** (red) and $CuCl_2$ (blue) in deionized water. Inset: magnified absorbance spectra of the visible region.

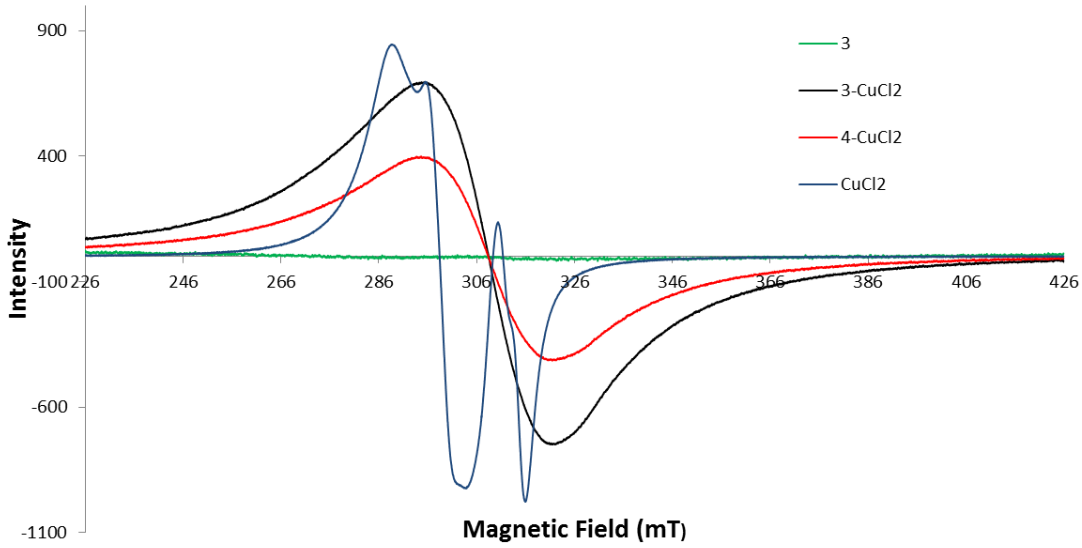

Fig. S22: Overlaid EPR spectra of polymer **3**, copper-complexed metallopolymers **3-$CuCl_2$** and **4-$CuCl_2$**, and $CuCl_2.5H_2O$ solid samples.

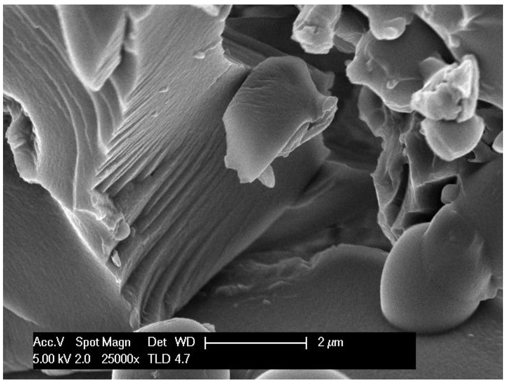

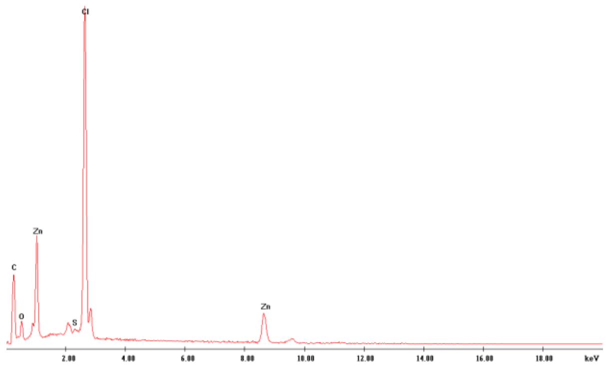

Fig. S23: (left) SEM image and (right) EDS spectrum of **3-$ZnCl_2$** metallopolymer precipitate.

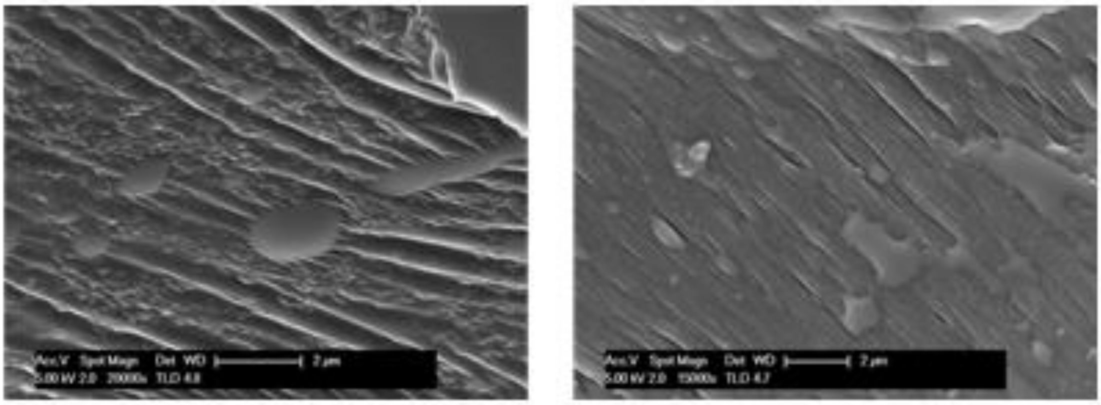

Fig. S24: SEM images (left) **3-CoCl$_2$** and (right) **3-CuCl$_2$** metallopolymer precipitates.

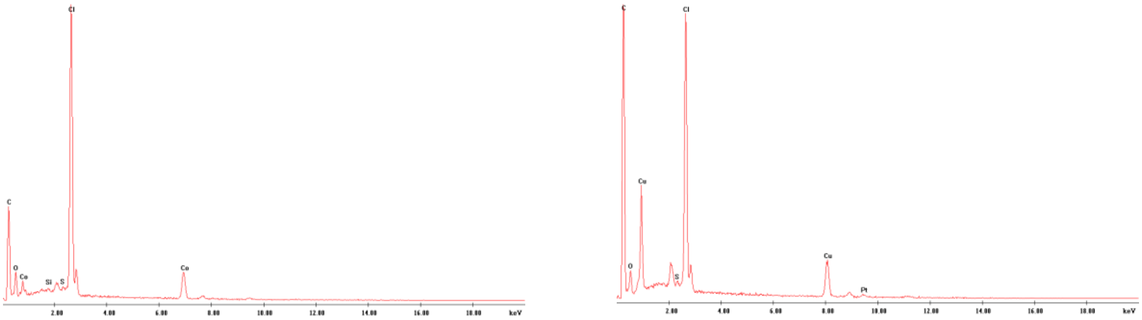

Fig. S25: EDS spectra of (left) **3-CoCl$_2$** and (right) **3-CuCl$_2$** metallopolymer precipitates.

Table S1: EDS results showing the relationship between the metal and Cl$^-$ anion for selected metallopolymers.

Metallopolymer	Atomic % of Metal	Atomic % of Cl$^-$	Atomic Ratio (Metal:Cl$^-$)
3-ZnCl$_2$	3.94	9.42	1 : 2
3-CoCl$_2$	1.99	7.46	1 : 3
3-CuCl$_2$	1.57	3.17	1 : 2
4-CuCl$_2$	4.43	8.08	1 : 2

(a) 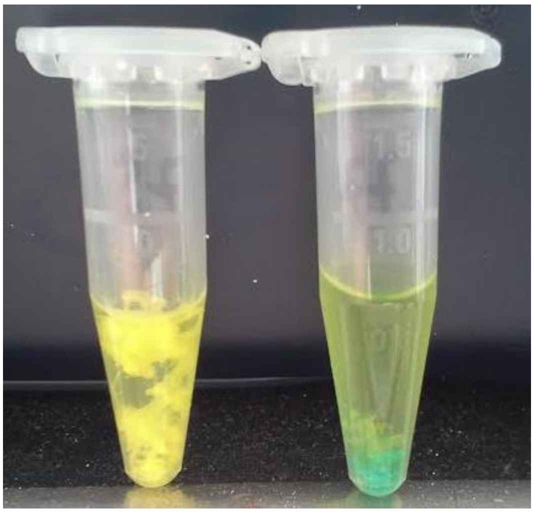 (b) 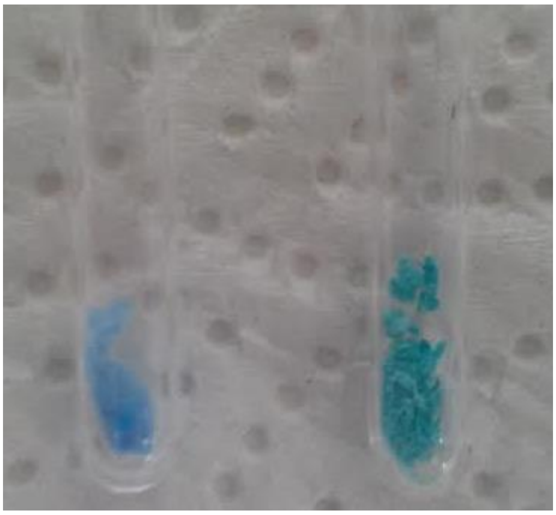

Fig. S26: Pictures of (a) methanol solution and (b) dried Cu-crosslinked-PAMAM (G0) (left) and Cu-crosslinked-5-PAMAM (G0) (right).

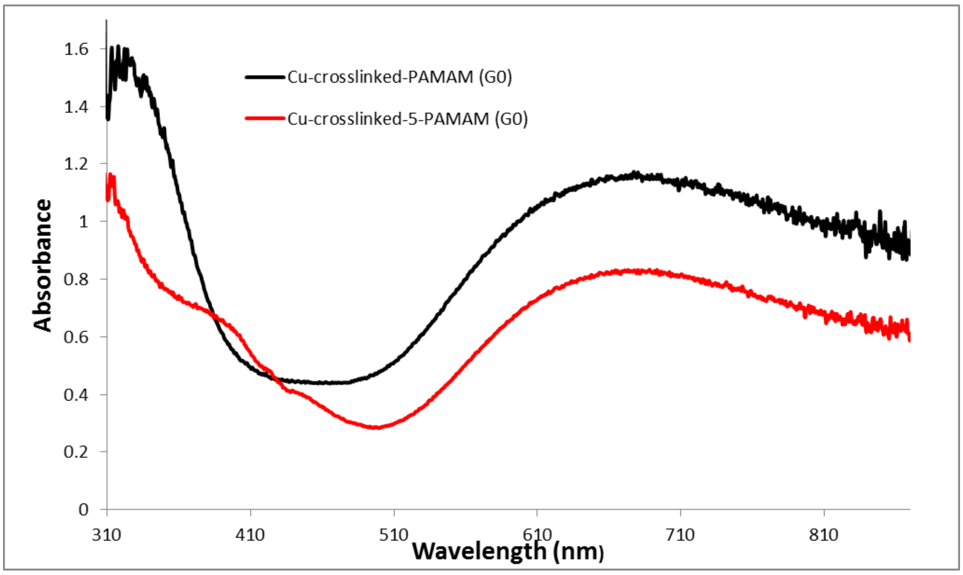

Fig. S27: Solid state UV-visible spectrum of copper complexed networks Cu-crosslinked-PAMAM (G0) (black) and Cu-crosslinked-5-PAMAM (G0) (red).